

Fig. 1. The block diagram of the first signal detection algorithm.

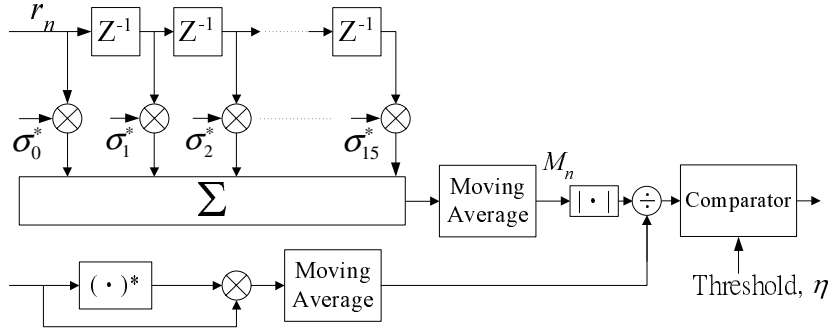


Fig. 2. The block diagram of the second signal detection algorithm.

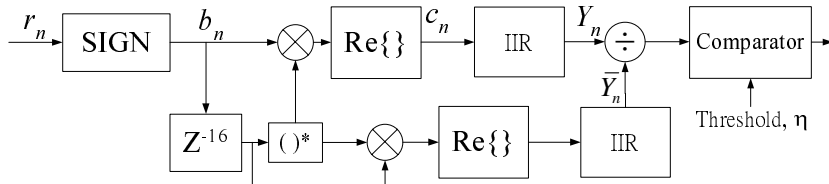


Fig. 3. The block diagram of the third signal detection algorithm.

the sequence that repeats r_{short} sequence 10 times. Therefore, this periodic characteristic is utilized for signal detection. In our computer simulation, (2) was used directly for signal detection instead of (1).

III. SIGNAL DETECTION ALGORITHMS

A. Three Signal Detection Algorithm

Based on the short training sequence shown in (2), three signal detection algorithms were designed and compared in the paper. The first algorithm [7][8] was designed based on the correlator structure, as shown in Fig. 1. The input sample was correlated with its delayed sample. According to the periodic characteristic, the delay amount was 16. After that, the correlated samples were averaged in the moving average block over a period of time L to suppress white noise, as shown below:

$$C_n = \sum_{k=0}^{L-1} r_{n-k} * r_{n-k-16}^* \quad (3)$$

$$= C_{n-1} + (r_n * r_{n-16}^*) - (r_{n-L} * r_{n-L-16}^*) \quad (4)$$

, where L was 32 in our design. The lower branch in Fig.1 was used to calculate the average energy of the received signal and to normalize the correlation output. Therefore, the correlation results were not affected by the signal with sudden peak. The normalized magnitude of C_n was taken and compared with a threshold, η . Finally, the received sample was claimed to be the OFDM symbol by the comparator block if \overline{C}_n was greater than η .

Fig. 2 showed the second signal detection algorithm, which was realized using the tapped delay line structure [9][10]. The input sample was matched with the 16 constant coefficients, as defined in (2), and averaged at the moving average block. The output of the matched filter, M_n , was expressed as below:

$$M_n = \sum_{i=0}^{15} r_{n-i} \sigma_i^* = \begin{cases} \sum_{i=0}^{15} |\sigma_i|^2, & \text{if matched} \\ 0, & \text{o.w.} \end{cases} \quad (5)$$

It was shown in (4) that a large correlation value was obtained if the input samples were matched. The lower branch in Fig.2 was also used for normalization. It was observed from Fig. 2 and (4) that the peak value of the normalized M_n at high signal-

to-noise-ratio (SNR) was about 1. Finally, the comparator block was utilized to determine the arrival of the OFDM symbols.

Fig. 3 showed the block diagram of the third signal detection algorithm. Only the sign of the input sample was taken for signal detection to simplify the hardware implementation. For example, $3.8 - j * 6.6$ was simplified to be $1 - j$. After that, the correlator structure in the first algorithm was used to calculate the correlation of the input samples. Since matched correlation value without noise was a real number, only the real part of the correlation value was used. Then, a first order infinite impulse response (IIR) filter with a leakage factor ($\alpha = 0.95$) was utilized to accumulate the correlation values for better performance

$$Y_n = \alpha * Y_{n-1} + (1 - \alpha) * \Re\{[r_n] * [r_{n-1}]^*\} \quad (6)$$

, where $[\]$ is the sign operator. Finally, a comparator with a constant threshold, η , was used to detect the OFDM burst.

B. Accumulation of the Correlation Values

In general, the performance of the signal detection algorithms in severe channel conditions is poor. To obtain reliable signal detection, the correlation outputs of signal detection algorithms were accumulated over several short training symbols. Therefore, C_n in (3) and M_n in (4) were summed up symbol-by-symbol, respectively. The decision was made after the accumulation. For the third signal detection algorithm, the accumulation mechanism was implemented within the algorithm and the accumulation length was determined by the leakage factor, which is more flexible. For practical implementation, most of the short training symbols (about 7 symbols) are utilized for AGC utilization. Only a small portion of the short training symbols are available for signal detection (about 3 symbols). Therefore, the valid accumulation length is about 2.4 us.

It is noted that the accumulation can also be implemented using the IIR filter structure for the first and the second signal detection algorithms.

C. Determination of Detection Threshold

The determination of detection threshold is the key parameter for correct signal detection. Due to the variation of the radio channel environment, the threshold should be set adaptively according to channel conditions. For the first signal detection algorithm, the average energy of the received signal calculated at the lower branch was used to determine the detection threshold. According to Fig. 1 and (3), the normalized correlation output at the receiver, R , was expressed as follows:

$$R \equiv \frac{P_U}{P_L} \quad (7)$$

$$= E\left[\frac{(r_n + w_n) * (r_{n-16} + w_{n-16})^*}{(r_n + w_n) * (r_n + w_n)^*}\right] \quad (8)$$

$$= \frac{\sigma_r^2}{\sigma_r^2 + \sigma_w^2} \quad (9)$$

$$= \begin{cases} \frac{SNR}{1+SNR} & , \text{if matched} \\ 0 & , \text{o.w.} \end{cases} \quad (10)$$

TABLE I
SUMMARY OF THE SIMULATION PARAMETERS

Simulation Parameters	Values
system	IEEE 802.11a
channel	AWGN
accumulation length	2.4 us
leakage factor	0.95
maximum decision threshold	0.5
minimum decision threshold	0.25
SNR Range	-10 ~ 0 dB

, where P_U was upper branch output and P_L was the lower branch output received. w_n was the additive white Gaussian noise (AWGN), σ_r^2 was the signal power, σ_w^2 was the noise power. According to (6) and (7), the noise power, σ_w^2 , was estimated at the lower branch of Fig.1 if there was no signal. Therefore, the detection threshold was given by

$$\eta = \begin{cases} 0.5 * \frac{P_U - P_L}{P_L} & , R \leq 0.5 \\ 0.25 & , R > 0.5 \end{cases} \quad (11)$$

According to (10), the detection threshold was set to be 0.25 when SNR was above 0 dB. On the other hand, the detection threshold was set based on the output of the upper and lower branches when SNR was below 0 dB.

The same approach was also applicable to the other two signal detection algorithms. It is noted that the detection threshold was updated every $0.8us$, which is the length of short training symbol.

IV. COMPUTER SIMULATION RESULTS

A series of Monte-Carlo simulations were conducted to evaluate the error detection probability of the three signal detection algorithms in AWGN channel. The parameters used in our computer simulation were summarized in Table I. The error detection probability was the sum of miss detection and false alarm probability. Fig. 4 compared the error detection probability, which was the sum of the miss detection and the false alarm probability, of the three signal detection algorithms in AWGN channel. It was shown that the second algorithm outperformed the other two algorithms. This was because the received samples were correlated with the pre-defined constants instead of its delayed versions. Therefore, less noise was introduced during the correlation process. However, the complexity of the second signal detection algorithm was much higher than the other two. On the other hand, the error detection probability of the third signal detection algorithm was higher than the other two. However, when SNR was 0 dB, the error detection probability of the third signal detection algorithm was below 10^{-2} .

Fig. 5 compared the average signal detection time required for the successful signal detection of these three signal detection algorithms when SNR is 0 dB, the average signal detection time of these three algorithms was below 2.4 us, which was the length of three short training symbols and met the design requirement. However, at very low SNR, the average signal detection time of the third algorithm increased fast. On the other

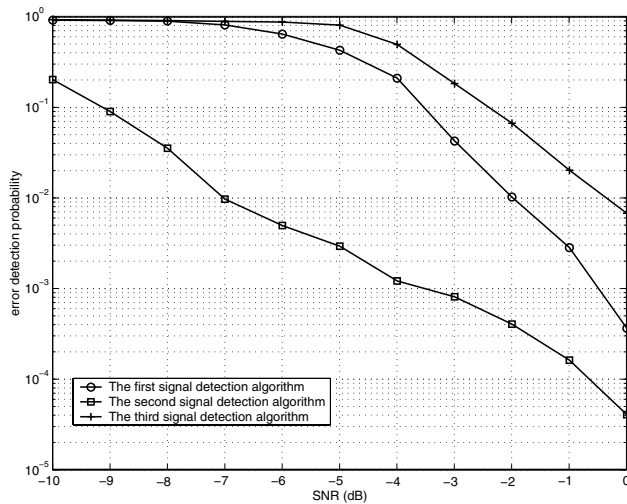


Fig. 4. Comparison of error detection probability of the three signal detection algorithms.

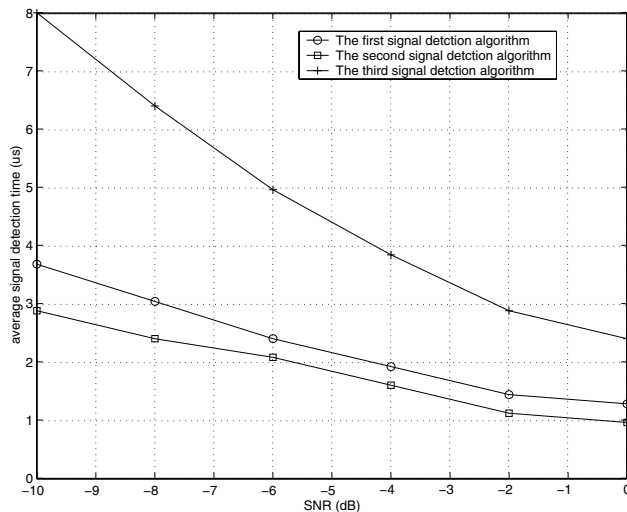


Fig. 5. Comparison of average signal detection time of the three signal detection algorithms.

hand, the average signal detection time of the first two algorithms were still below 2.4 us when SNR was -6 dB. Therefore, the first two signal detection algorithms were reliable at very low SNR.

The implementation complexity was evaluated using TI C6201 evaluation board. The clock cycles required to determine whether the current input sample was an OFDM symbol were measured using the Profiler tool of TI code composer studio (CCS) with level 3 optimization. According to our evaluation, the clock cycles required to calculate each input sample correlation for these three algorithms were 76, 846, and 18, respectively, as shown in Table II. It was shown that the complexity of the second signal detection algorithm was much higher than the other two algorithms, though the error detection probability was the lowest.

TABLE II
SUMMARY OF THE COMPLEXITY OF THE SIGNAL DETECTION ALGORITHMS

Signal Detection Algorithm	1	2	3
Complexity (clock cycles/sample)	76	846	18

V. CONCLUSIONS

We designed and compared three signal detection algorithms for IEEE 802.11a WLAN system. The periodicity characteristic of the short training sequence was utilized. It was shown in our simulations that the second signal detection algorithm outperformed the other two with the highest complexity. On the other hand, the third algorithm was the most suitable structure for hardware implementation with the lowest complexity when SNR was above 0 dB. Though its performance was poor at very low SNR, the error detection probability was below 10^{-2} when SNR was above 0 dB. Practical system implementation is a compromise between the performance and the complexity requirements. The clock recovery (sampling points), fixed point implementation, and bits resolution issues will be considered in the future works.

REFERENCES

- [1] S. B. Weinstein, P. M. Ebert, "Data transmission by frequency division multiplexing using the discrete Fourier transform," *IEEE Trans. Commun.*, Oct. 1971, Vol. COM-19, pp. 628-634.
- [2] W. Y. Zou and Y. Wu, "COFDM: An overview," *IEEE Trans. Broadcasting*, vol. 41, pp. 1-8, Mar. 1995.
- [3] T. Ojanpera and R. Prasad, "An Overview of wireless broadband communications," *IEEE Commun. Mag.*, vol. 35, pp.28-34, Jan. 1997.
- [4] M. Speth, D. Daecke, and H. Meyr, "Minimum overhead burst synchronization for OFDM based broadband transmission," in *IEEE Proc. Globecom'98*, pp. 3227-3232 1998.
- [5] IEEE 802.11a, "Wireless LAN medium access control(MAC) and physical layer(PHY) specifications: high-speed physical layer in the 5 GHz band", IEEE Std 802.11a, 1999.
- [6] J. Heiskala and J. Terry, *OFDM wireless LANs: A Theoretical and Practical Guide*, SAMS, Indiana, 2001.
- [7] D. C. Schmidl and D. C. Cox, "Low-overhead, low-complexity [burst] synchronization for OFDM," in *IEEE Proc. ICC'96*, Vol. 3, pp. 1301-1306, 1996.
- [8] J. J. van de Beek, M. Sandell, M. Isaksson, and P. O. Borjesson, "ML estimation of time and frequency offset in OFDM systems," *IEEE Trans on Signal Processing*, Vol. 45, No. 7, pp. 1800-1805, July, 1997.
- [9] B. Yang, K. B. Letaief, R. S. Cheng, and Z. Cao, "Robust and improved channel estimation for OFDM systems in frequency selective fading channels," in *IEEE Proc. Globecom'99*, pp.2499-2503.
- [10] M. Speth, F. Classen, and H. Meyr, "Frame synchronization of OFDM systems in frequency selective fading channel," in *IEEE Proc. VTC'97*, pp.1807-1811, Phoenix AZ U.S.A., May 1997.